Optik 122 (2011) 136–141

Contents lists available at ScienceDirect

Optik

journal homepage: www.elsevier.de/ijleo

Characterization of the train-average time–frequency parameters inherent in the low-power picosecond optical pulses generated by the actively mode-locked semiconductor laser with an external single-mode fiber cavity

Alexandre S. Shcherbakov[a,*], A.Yu. Kosarsky[b,2], Pedro Moreno Zarate[a,1], Joaquin Campos Acosta[c,3], Yurij V. Il'in[d,4], Il'ya S. Tarasov[d,4]

[a] Department of Optics, National Institute for Astrophysics, Optics, and Electronics (INAOE), A.P. 51 and 216, Puebla, Pue. 72000, Mexico
[b] LLC Petro, Peterhoff Chausse 71, Saint-Petersburg 198206, Russian Federation
[c] Department of Metrology, Institute for Applied Physics (IFA-CSIC), Serrano 144, Madrid 28006, Spain
[d] A.F.Ioffe Physical-Technical Institute of the Russian Academy of Sciences, Polytechnicheskaya St. 26, Saint-Petersburg 194021, Russian Federation

ARTICLE INFO

Article history:
Received 25 June 2009
Accepted 27 November 2009

Keywords:
Semiconductor laser
Active mode-locking
Wigner time–frequency distribution
Train-average parameters

ABSTRACT

The specific approach to characterizing the train-average parameters of low-power picosecond optical pulses with the frequency chirp, arranged in high-repetition-frequency trains, in both time and frequency domains is elaborated for the important case when the semiconductor laser is matched by an external single-mode fiber cavity and operates in the active mode-locking regime. This approach involves the joint Wigner time–frequency distributions, which can be created for those pulses due to exploitation of a novel interferometric technique. Practically, the InGaAsP/InP-heterolaser generating at the wavelength 1320 nm was used during the experiments carried out and an opportunity of reconstructing the corresponding joint Wigner time–frequency distributions was successfully demonstrated.

© 2010 Elsevier GmbH. All rights reserved.

1. Introduction

We present an approach to the characterization of low-power bright picosecond optical pulses with an internal frequency modulation in both time and frequency domains in practically important case of exploiting the semiconductor laser matched by a single-mode optical fiber and operating in a near-infrared range in the active mode-locking regime [1]. This approach uses the joint Wigner time–frequency distributions [2], which can be found for this regime due to involving a novel original interferometric technique [3]. In so doing, the modified scanning Michelson interferometer was chosen for shaping the field-strength auto-correlation functions peculiar to the pulsed infrared light radiation. We exploit the key features of this experimental technique for accurate and reliable measurements of the train-average temporal width and the frequency chirp associated with picosecond optical pulses in high-repetition-rate pulse trains. This technique is founded on an ingenious algorithm elaborated specially for the advanced optical metrology, which makes possible constructing the joint Wigner distributions and describing the above-listed parameters of optical pulses. The InGaAsP/InP-heterolaser, operating at 1320 nm range, with about one meter length external single-mode silicon fibers was exploited during the experiments carried out. When the optical signal consisted of contiguous pulses with the repetition frequency close to 1 GHz, due to operating semiconductor laser in the active mode-locking regime, typical pulse train-average auto-correlation function had been characterized by temporal widths just in picosecond range. The accuracy of similar measurements increased with growth of the repetition frequency due to rising in a number of samples.

2. The joint Wigner time–frequency distribution

This consideration is directly related to the analysis of signals, which are non-stationary in behavior in time and frequency domains. The main problem here is connected with finding a joint function of both the time and the frequency, i.e. some distribution, which will be able to describe the energy density or the intensity of an arbitrary signal in terms of time and frequency simultaneously. Ideally, it would be an analytic function of two arguments

* Corresponding author. Tel.: +52 222 2472940; fax: +52 222 2472940.
E-mail addresses: alex@inaoep.mx (A.S. Shcherbakov), alexey.kosarsky@jt-int.com (A.Yu. Kosarsky), pemzamx@gmail.com (P.M. Zarate), joaquin.campos@ita.cetef.csic.es (J.C. Acosta), ptk@mail.ioffe.ru (Y.V. Il'in), tarasov@hpld.ioffe.ru (I.S. Tarasov).
[1] Tel.: +52 222 2472940; fax: +52 222 2472940.
[2] Tel.: +7 812 534 3334.
[3] Tel.: +34 915618806; fax: +34 914117651.
[4] Tel.: +7 812 292 7379/7997.

0030-4026/$ – see front matter © 2010 Elsevier GmbH. All rights reserved.
doi:10.1016/j.ijleo.2009.11.020

having properties of the density function, which characterizes the energy, or intensity, of a signal at unity time interval as well as at unity frequency interval. Together with this, it should be noted that time–frequency analysis exhibits a row of peculiarities; for example, it is governed by the uncertainty principle. Introducing similar joint time–frequency distribution $P(t, \omega)$, one can write:

$$\int_{-\infty}^{\infty} P(t,\omega)\,d\omega = |A(t)|^2, \tag{1a}$$

$$\int_{-\infty}^{\infty} P(t,\omega)\,dt = |S(\omega)|^2, \tag{1b}$$

where $A(t)$ and $S(\omega)$ are the amplitude of a determined signal and its Fourier transform, respectively, so that

$$S(\omega) = 1/2\pi \int_{-\infty}^{\infty} A(t)\exp(-i\omega t)\,dt.$$

The total energy can be determined as

$$W_0 = \int_{-\infty}^{\infty}\int_{-\infty}^{\infty} P(t,\omega)d\omega\,dt = \int_{-\infty}^{\infty} |A(t)|^2 dt = \int_{-\infty}^{\infty} |S(\omega)|^2 d\omega, \tag{2}$$

if the conditions for existing both the corresponding one-dimensional distributions are satisfied. It follows from the basic mathematical principles that an uncertainty principle characterizes the fundamental coupling between a root-mean-square deviation of some function and a root-mean-square deviation of Fourier-transform peculiar to the same function. In the particular case of a pair including $A(t)$ and $S(\omega)$, these root-mean-square deviations in time and frequency domains can be determined by

$$\tau_{SA} = \sqrt{T_2 - (T_1)^2}, \tag{3a}$$

$$T_n = W_0^{-1} \int_{-\infty}^{\infty} t^n |A(t)|^2\,dt, \tag{3b}$$

$$\omega_{SA} = \sqrt{\omega_2 - (\omega_1)^2}, \tag{4a}$$

$$\omega_n = W_0^{-1} \int_{-\infty}^{\infty} \omega^n |S(\omega)|^2\,d\omega. \tag{4b}$$

The corresponding uncertainty principle is given by the relation $\tau_{SA} \cdot \omega_{SA} \geq 1/2$. In context of the determined functions, this relation means that the determined function and its Fourier transform cannot have simultaneously arbitrary small widths. In its turn, in the signal analysis, where τ_{SA} has a meaning of the root-mean-square time duration and ω_{SA} has a meaning of the root-mean-square spectral width, this fact speaks that the signal and its spectrum cannot have simultaneously arbitrary small widths as well. There are a few options to choose a concrete form of the joint time–frequency distribution. In particular, one can take the Wigner time–frequency distribution, i.e. assume that $P(t, \omega) = W(t, \omega)$, which is given by, see for example [2]:

$$W(t,\omega) = \frac{1}{2\pi}\int_{-\infty}^{\infty} A^*\left(t - \frac{\tau}{2}\right)\exp(-i\tau\omega)A\left(t + \frac{\tau}{2}\right)d\tau$$

$$= \frac{1}{2\pi}\int_{-\infty}^{\infty} S^*\left(\omega - \frac{\theta}{2}\right)\exp(it\theta)S\left(\omega + \frac{\theta}{2}\right)d\theta. \tag{5}$$

The kernel of this distribution depends on the product of its arguments. Theoretically, the Wigner distribution has an infinite resolution in time due to absence of averaging over any finite time interval. Moreover, for finite lag length, it has an infinite frequency resolution. Together with this, the Wigner distribution being quadratic in nature is able to introduce various cross terms for a multi-component signal.

The complex amplitude of a solitary optical pulse with the Gaussian shape of envelope can be written as

$$A_G(t) = A_0 \exp\left[-\frac{(1+ib)t^2}{2T^2}\right], \tag{6}$$

where A_0 is the real-valued amplitude, T is the Gaussian pulse half-width measured at a level of $1/e$ for the intensity contour and b is the parameter of frequency modulation, i.e. the frequency chirp. In this case, the joint Wigner time–frequency distribution, see Eq. (5), inherent in a Gaussian pulse with $A_0 = 1$ is given by

$$W_G(t,\omega) = \frac{T}{\sqrt{\pi}}\exp\left[-\frac{t^2}{T^2} - \left(\omega T + \frac{bt}{T}\right)^2\right]. \tag{7}$$

The Wigner distribution (7) for the Gaussian pulse is positive-valued. When $T = 1$ and $b = 0$, Eq. (7) gives the distribution, which is symmetrical relative to repositioning the variables t and ω. With decreasing the parameter b, the energy distribution concentrates in a bandwidth corresponding to the chirp-free spectrum (i.e. to the transform limited pulse) whose center lies along the line $\omega = bt/T^2$. Two illustrative examples of the time–frequency distribution $W_G(t, \omega) = \pi^{-1/2}\exp[-t^2 - (\omega + bt)^2]$, defined by Eq. (7) with $T = 1$ and $b = 0, 2$ are presented in Fig. 1. One can see that a contribution of the frequency chirp gives mainly rotating the Wigner distribution on the (t, ω)-plane.

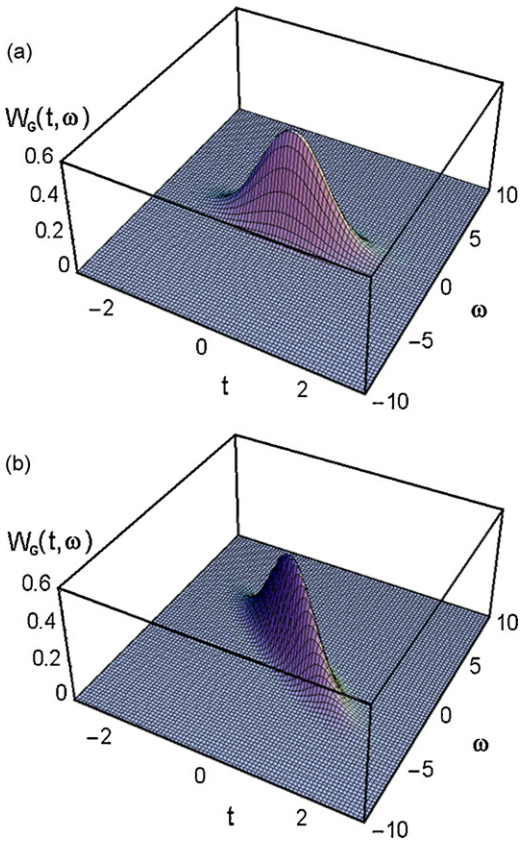

Fig. 1. Two examples of typical Wigner time–frequency distributions for the Gaussian pulses with $T = 1$ and the varying parameter b: (a) $b = 0$ and (b) $b = 2$.

Integrations of Eq. (7) give the partial one-dimensional Wigner distributions for a Gaussian pulse over the time or frequency separately:

$$|A_G(t)|^2 = \int_{-\infty}^{\infty} W_G(t,\omega)\,d\omega = \exp\left(-\frac{t^2}{T^2}\right), \tag{8a}$$

$$|S_G(\omega)|^2 = \int_{-\infty}^{\infty} W_G(t,\omega)\,dt = \frac{T^2}{\sqrt{1+b^2}}\exp\left(-\frac{T^2\omega^2}{1+b^2}\right). \tag{8b}$$

It is seen from Eq. (8b) that to reach a level of $1/e$ one need vary the variable ω from $-T^{-1}\sqrt{1+b^2}$ to $T^{-1}\sqrt{1+b^2}$, so that the variation $\Delta\omega = T^{-1}\sqrt{1+b^2}$ means actually the half-width of the spectral contour at a level of e^{-1}. Thus, one can determine the product:

$$\Delta\omega T = \sqrt{1+b^2}. \tag{9}$$

In the particular case of $b = 0$ (i.e. in the absence of the frequency chirp or the phase modulation), one yields $\Delta\omega T = 1$ for a Gaussian pulse. Nevertheless, $b \gg 1$ in general case, so that the product $\Delta\omega T$ can far exceed unity.

3. Measuring the train-average parameters of picosecond optical pulses with Gaussian shape in high-repetition-rate trains

When simple method is required for measuring current time–frequency parameters of low-power pico- and sub-picosecond optical pulses traveling in high-repetition-rate trains, a method based on forming a train-average auto-correlation function of the field-strength, which is coupled through the Fourier transform with the spectral power density, can be exploited. From the recorded power spectral density, one can determine an average width of the radiation spectrum. However, in this case, information on the average field phase is lost and one cannot determine the time variation of the field amplitude $A(t)$. Exact determination of the train-average pulse duration from the width of the radiation spectrum is only possible when the shape of pulse envelope is known a priori and, in addition, the pulse spectrum is transform limited in behavior [4]. An approximate estimation of the pulse duration is also correct, if the frequency chirp is sufficiently small [5]. Here, we use an opportunity [3] of providing experimental conditions, under which the train-average auto-correlation function of the field-strength can serve as a source of exact and reliable information on the average values of both duration and frequency chirp of a low-power optical pulses traveling in high-repetition-rate trains. As usually, let us proceed from the assumption that all pulses in a train are identical pulses with a Gaussian envelope, see Eq. (6), with the amplitude $A_0 = \sqrt{P}$, where P is the incoming pulse peak power. As it was listed above for a Gaussian envelope, the relationships between the train-average pulse parameters T and b and the width τ_0 of the corresponding auto-correlation function, measured on a level of $1/e$ for the intensity contour, are given by

$$\tau = \tau_0 = \frac{2T}{\sqrt{1+b^2}} \tag{10}$$

Usually, the real-time auto-correlation function of the field-strength averaged over a train of optical pulses is obtained with a scanning Michelson interferometer [5,6], which allows measuring the value of τ_0. However, information on the width τ_0 of the field-strength auto-correlation function is insufficient to determine the time–frequency parameters of pulse train. That is why one can propose performing two additional measurements of the auto-correlation function width with the help of a scanning Michelson interferometer. During the second and third measurements, supplementary optical components, changing the parameters T and b in a predetermined way but not influencing the envelope of the investigated pulses, should be placed in front of the beam-splitting mirror of the interferometer. The auto-correlation function widths τ_m $(m = 1, 2)$ obtained from the repeated measurements are coupled with the new values of the pulse duration T_m and the frequency chirp b_m by Eq. (10). One can assume that $T_m = \alpha_m T_0$ and $b_m = b_0 + \beta_m$, where T_0 and b_0 are unknown values of the parameters T and b, while the quantities α_m and β_m are determined by supplementary optical components. Using the above-noted relations, one can write two different algebraic quadratic equations for a quantity of b_0. The corresponding solutions are given by a pair of the following formulas:

$$b_0 = (q_m\alpha_m^2 - 1)^{-1}[\beta_m \pm \sqrt{q_m\alpha_m^2(\beta_m^2+2) - (q_m^2\alpha_m^4+1)}], \tag{11}$$

where $q_m = \tau_0^2/\tau_m^2$ and τ_m is the width of the field-strength auto-correlation function obtained without supplementary optical components. For $(m = 1, 2)$, Eq. (11) gives four values of b_0, of which two coincide with each other and correspond to just the true value of the train-average frequency chirp of the pulses. This method of measuring allows one to determine both the value and the sign of the frequency chirp, which is often impossible even with the help of substantially more complicated methods, such as, for example, the method described in [7]. Once the pulse frequency chirp b_0 is determined, one can use formula (11) to calculate the pulse duration T by using τ_0 and $b = b_0$. For the supplementary electronically controlled optical component, one can propose exploiting a specific device based on an InGaAsP/InP single-mode traveling-wave semiconductor heterolaser, which is quite similar to a saturable-absorber laser with the clarified facets [3,8].

4. Experimental studies

Semiconductor lasers have a broad gain band (about $\Delta\nu \approx 10^{13}$ Hz), so that by this is meant that their operation in the regime of active mode-locking makes it possible to expect generating ultrashort optical pulses with a duration of about $\tau_0 \approx 1/\Delta\nu$ lying in a picosecond time range. Generally, the active mode-locking process provides shaping stable trains of wave packets with rather good reproducibility from pulse to pulse. Recently, this regime has been practically realized utilizing a periodic modulation of gain inherent in the active medium through injecting the pump current with a frequency equal or multiple to the frequency spacing between longitudinal modes of the laser cavity. Within this discussion, the single-mode InGaAsP/InP semiconductor laser is considered. It has been designed with one antireflection-coated facet and matched by an external single-mode optical fiber cavity. To obtain the shortest possible optical pulses the facet of semiconductor crystal facing the fiber cavity were coated via deposition of a SiO_2-film, so that the reflection coefficient was typically less than 1%. An external cavity was made of a single-mode silica optical fiber with the refractive index $n \approx 1.5$ and the length $L \approx 1$ m with an additional mirror at its far end, providing the optical feedback. The corresponding feedback factor was estimated by 15% due to about 40%-efficiency of exiting the light radiation in that optical fiber by semiconductor laser structure with the refractive index $n_S \approx 3.3$. The fiber cavity length L corresponded to the frequency spacing about $f_0 \approx 100$ MHz between its longitudinal optical modes because of $f = c/(2n)$, where c is the light velocity. The scheme of our experiments is presented in Fig. 2.

Periodic modulation of optical losses in a cavity was provided through modulating the pump current from an external

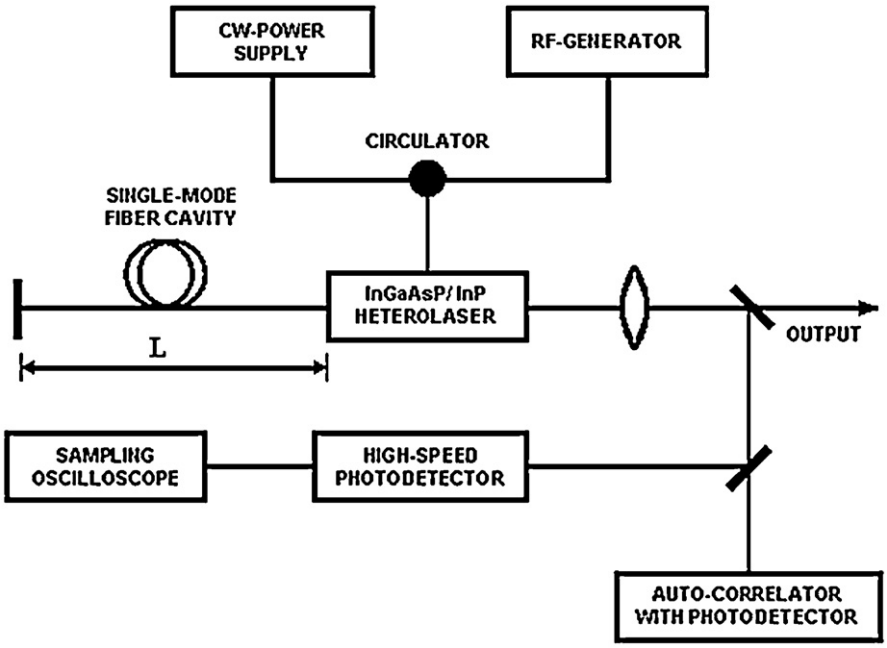

Fig. 2. Schematic arrangement of the experimental set-up.

source of the electronic sinusoidal RF-signal within the frequency range 400–800 MHz. The electronic port of semiconductor laser was matched with a 50-Ohm output of that source via specially designed strip-line waveguiding circuit. The regular operation of semiconductor laser was provided by thermo-stabilizing system at a temperature of 16 °C with an accuracy of ±0.2 °C. The regime of operation was controlled by the diffractive optical spectrometer. Fig. 3 illustrates profiles of light radiation spectra at the wavelength $\lambda = 1320$ nm without an external RF-modulation as well as with periodic RF-modulation applied at the semiconductor laser, i.e. in the active mode-locking regime. The extended spectrum width within the active mode-locking regime was estimated by about $\Delta\lambda \approx 100$ Å. In the frequency domain, this estimation gives $\Delta\nu = (\Delta\lambda)c/\lambda^2 \approx 1.72$ THz that makes it possible to expect generating trains of ultra-short optical pulses with characteristic durations lying in the picosecond range. A bit rugged profile inherent in the spectrum in Fig. 3b is affected evidently by the presence of the laser diode cavity by itself and connected with residual reflections from the coated diode facet, which is facing the fiber cavity.

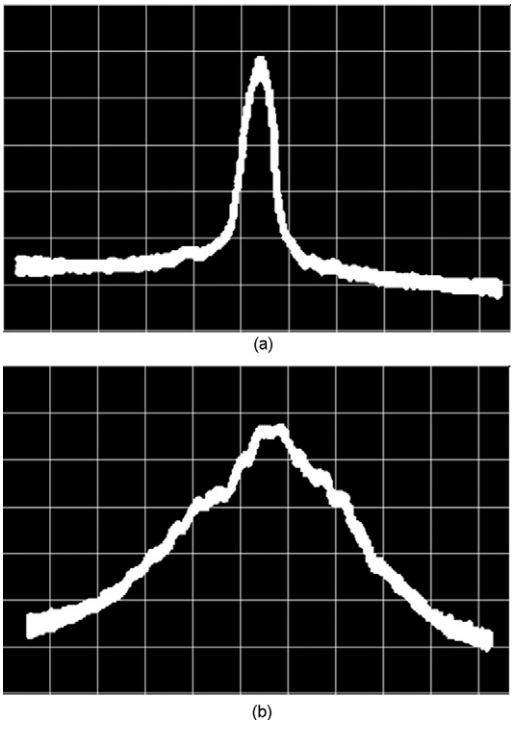

Fig. 3. Radiation spectra inherent in semiconductor laser operating at the wavelength $\lambda = 1320$ nm: (a) without an external modulation; (b) with an external sinusoidal modulation, i.e. in the active mode-locking regime.

Measuring the time–frequency parameters of optical pulses was carried out exploiting the interferometric technique described in [3]. At first, our experimental studies have demonstrated that within mode-locking a single-mode InGaAsP-laser heterostructure at a threshold of self-excitation (practically, it was realized at a pump current of about 50 mA), only a spike-mode free oscillation regime had been observed with an individual spike width of about 0.7–0.9 ps. The investigation of these spikes has shown that each individual spike includes an irregular set of intensity fluctuations. Fig. 4 represents an example of the digitized oscilloscope trace for the auto-correlation function related to a spike-mode free oscillation when an average spike width is close to 0.7 ps.

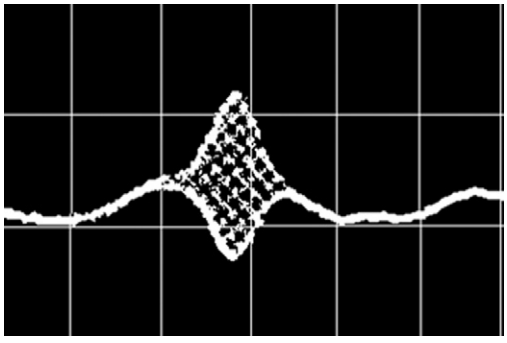

Fig. 4. The digitized oscilloscope trace for the auto-correlation function for a spike-mode free oscillation with an average spike width of about 0.7 ps.

Then, during the performed proof-of-principle experiments, we had shaped stable trains of rather powerful (about 1 W in a peak) picosecond optical pulses with predictable pulse parameters and with the repetition frequency multiple to the frequency spacing of longitudinal optical modes in fiber cavity. An opportunity had been used of estimating the train-average pulse duration as well as the train-average frequency chirp. Shaping a continuous-wave sequence of stable regular ultra-short optical pulses with duration of about 2–10 ps can be achieved only after exceeding a threshold of self-excitation by 10–20%. In so doing, one can observe increasing the energy of oscillation about 10 times, so that the peak power of regular optical pulses approaches 0.2–1.0 W. The active mode-locking regime on multiple repetition frequencies can be associated with the cases of circulating more than one optical pulse in a long-haul cavity. A number of the circulating optical pulses N can be estimated as $N = 2nfL/c$, and experimentally the cases with $N = 1 - 8$ had been successfully realized. It can be noted that the interferogram widths, measured on a level of $1/e$ for the intensity contour, were decreasing from 12.2 to 3.9 ps as the number N was growing from 1 to 8. The absolute frequency bandwidth, being available for the observation of mode-locking, was varying in the range 0.2–0.5 MHz, so that the relative frequency locking band was a little bit less than 10^{-3}. Fig. 5a represents the digitized interferogram of the second order auto-correlation function for a high-repetition-rate train of optical pulses; the width of this interferogram was estimated by 4.4 ps, while Fig. 4b shows the digitized oscilloscope trace for a train of ultra-short pulses with the repetition frequency $f \approx 7f_0 = 718$ MHz, which was identified as the most stable during the experiments performed. The parameter b, related to the frequency chirp, was estimated with applying the above-mentioned technique by $b \approx 1.46 \times 10^{-4}$. This is a train of picosecond pulses detected with the time resolution of about 300 ps, which is associated with the transfer function of a high-speed photodetector exploited. The off-duty ratio for optical pulses depicted in Fig. 5b is in correspondence to the ration between the repetition period $1/f$ and the above-mentioned time resolution of that high-speed photodetector.

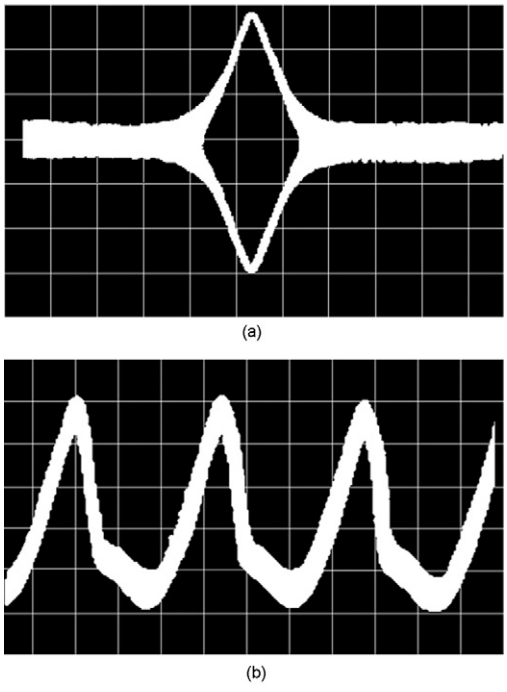

Fig. 5. The digitized oscilloscope traces related to a regular pulse train: (a) the train-average auto-correlation function; the pulse width of this interferogram, measured on a level of $1/e$ for the intensity contour, was estimated by 4.4 ps; (b) the output signal from a high-speed photodetector; a train of the same ultra-short optical pulses with the repetition frequency $f \approx 718$ MHz was detected with the time resolution of about 300 ps.

5. Characterizing optical pulses

Within the direct photodetection, the time resolution is restricted by inertia of various components and an effect of storage associated with this inertia [6]. The response function $R(t)$, inherent in even rather high-speed photodetector, is not perfectly identical to the incoming optical signal $S(t)$, because this response is conditioned by a transfer function $B(t)$. As a result, one has to write:

$$R(t) = \int_{-\infty}^{\infty} dt_1 S(t_1) B(t_1 - t), \tag{12}$$

in linear systems. Moreover, $B(t_1 - t) = 0$ with $t_1 > t$ due to the causality principle. One can see that the response function $R(t)$ is coinciding with the signal $S(t)$ only if the transfer function $B(t)$ is the Dirac δ-function. Usually, the normalized transfer functions of high-speed photodiodes can be mathematically approximated by functions of two kinds, namely, by the exponential function $\exp(-t/T)$ or the hyperbolic-like function $[1 + (t/T)^m]^{-1}$ with the power $m \in [1, 2]$, where the characteristic parameter T is determined by properties of each individual type of photodetectors. Fig. 6 illustrates principally appearing the response function conditioned by the incoming ultra-short Gaussian optical pulse and the exponential transfer function.

In the active mode-locking regime, optical pulses are self-reproducing after each path through the cavity. Restoration of pulse parameters is conditioned by properties of the active medium, and because the cavity exhibits an optical dispersion, one of the necessary conditions for reproducibility of pulses is the presence of frequency chirp. Presently known mechanisms of interacting optical pulses with semiconductors allow us to simplify the theoretical model of shaping an ultra-short pulse with the complex field amplitude $E(t) = A(t)\exp(i\omega_0 t) + c.c.$ in a heterostructure. The pulse, grown during the process of active mode-locking, has a Gaussian shape and can be described by Eq. (11). The pulse width, measured on a level of $1/e$ for the intensity contour, is given by [8]:

$$T = (gm)^{-1/4}(\omega_m \omega_S)^{-1/2}, \tag{13}$$

where g is the maximal gain at $t = 0$, m is the factor of external modulation of the losses in a cavity, ω_m is the external modulation frequency, and ω_S is the gain contour width. Finally, the frequency chirp can be expressed as [8]:

$$b = 2T^2\beta, \tag{14a}$$

$$\beta = \frac{L_D \omega_m \omega_S^2 \sqrt{m}}{4[g\omega_0 T_C/(2Q)]^{3/2}} \left(\frac{d^2k}{d\omega^2}\right), \tag{14b}$$

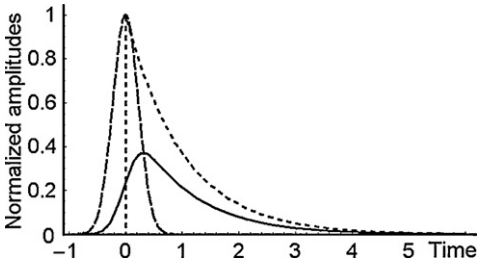

Fig. 6. Shaping the response function (solid line) conditioned by the incoming ultra-short Gaussian optical pulse (dashed line) and the exponential transfer function (dotted line); the scales of curves are changed to illustrate better.

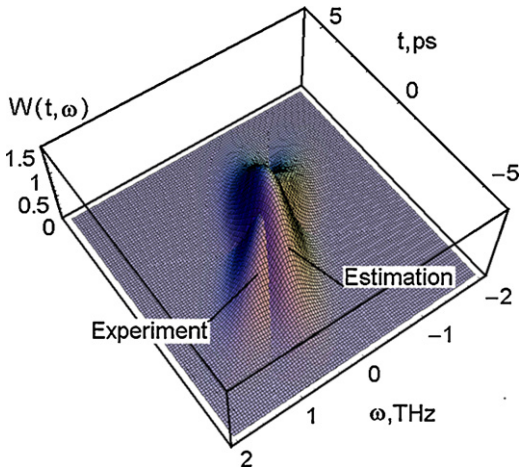

Fig. 7. A pair of the Wigner time–frequency distribution for the Gaussian pulses obtained from the performed estimation with $T = 2.73$ ps and the $b = 0.84 \times 10^{-4}$ as well as from the experiment with $T = 2.2$ ps and the $b = 1.46 \times 10^{-4}$.

where β is the dimensional factor of frequency chirp, L_D is the length of high-dispersion components (for example, the laser crystal), ω_0 is the central frequency of emission, Q is the quality factor inherent in a cavity, T_C is the transit time of a pulse through a cavity, and k is the wave number. In fact, Eqs. (13) and (14) can be practically used to estimate the parameters of the optical pulses generated.

Using the values characteristic of the experiments: $g = 3$, $m = 0.25$, $\omega_m = 2\pi \times 718 \times 10^6$ rad/s, and $\omega_S = 2\pi \times 10^{13}$ rad/s, one can obtain $T \approx 2.73$ ps from Eq. (13), which can be considered as rather good agreement with the experimental data. The frequency chirp that arises within establishing the self-reproducing pulses can be estimated with Eq. (14). For $L_D \approx 0.5$ mm, $\omega_0 = 2.1 \times 10^{15}$ rad/s (at $\lambda = 1320$ nm), $T_C = 10^{-8}$ s, $Q = 10^5$, and $(d^2k/d\omega^2) = 3.7 \times 10^{-24}$ s^2/m, one can obtain $\beta = 7.3 \times 10^{18}$ s^{-2} from Eq. (14b). Nevertheless, this dimensional magnitude of the estimated frequency chirp is relatively small, because one can find from Eq. (14a) in dimensionless values that $b \approx 0.84 \times 10^{-4} \ll 1$. In practically reasonable assumption that the envelopes of optical pulses under consideration can be described rather adequately by Gaussian functions, these estimations make it possible to create the corresponding theoretical version of Wigner time–frequency distribution with the above-calculated parameters T and b. Together with this, the experimental version of similar time–frequency distribution can be designed with experimentally obtained parameters $T \approx 2.2$ ps and $b \approx 1.46 \times 10^{-4}$ in the same approximation by Gaussian functions. The resulting plots of two Wigner distributions for the Gaussian-like optical pulses, obtained from estimations and from experiment, are shown in Fig. 7.

6. Conclusion

A novel approach to the characterization of low-power bright picosecond optical pulses with an internal frequency modulation in both time and frequency domains in practically important case of operating the semiconductor laser with an external single-mode fiber cavity in near-infrared range in the active mode-locking regime has been presented. This approach is oriented to using the joint Wigner time–frequency distributions. Similar distributions can be created for this regime within exploiting the progressed interferometric technique briefly described above. The modified scanning Michelson interferometer has been chosen for obtaining the field-strength auto-correlation functions. In fact, we have presented the key features of a new experimental technique for accurate and reliable measurements of the train-average temporal width and the frequency chirp of picosecond optical pulses in high-repetition-rate trains. This technique makes it possible to find the parameters needed for reconstructing the joint Wigner distributions inherent in optical pulses. The InGaAsP/InP-heterolaser, operating at 1320 nm wavelength range, has been used within the experiments. When the optical signal consists of contiguous pulses with the repetition frequency close to 1 GHz, conditioned by operating semiconductor laser in the active mode-locking regime, typical requirements for measurements and operating with the Wigner distributions have been satisfied, so that the train-average pulse parameters have been successfully characterized.

Acknowledgement

This work has been financially supported by the CONACyT, Mexico (project #61237-F). The authors thank I. A. Kniazev and I. E. Berishev for their remarkable contribution to the proof-of-principle experiments carried out Dra. A Pons Aglio (IFA-CSIC) for discussing the problems of the photo-detecting.

References

[1] G.P. Agrawal, N.K. Dutta, Semiconductor Lasers, 2nd ed., Van Nostrand Reinhold, New York, 1993.
[2] L. Cohen, Time–frequency distributions—a review, Proc. IEEE 77 (1989) 941–981.
[3] A.S. Shcherbakov, A.L. Munoz Zurita, A.Yu. Kosarsky, J. Campos Acosta, Determining the time–frequency parameters of low-power bright picosecond optical pulses using interferometric technique, OPTIK—Int. J. Electron. Opt. (Elsevier, Germany) 121 (2010) 426–434.
[4] E.P. Ippen, C.V. Schenk, Picosecond techniques and applications, in: S. Shapiro (Ed.), Ultrashort Light Pulses, Springer, Heidelberg, 1977.
[5] A.S. Shcherbakov, Synchronization of a radio-interferometer by the high-repetition-rate picosecond solitons, Tech. Phys. Lett. 19 (1993) 615–616.
[6] J. Herrmann, B. Wilhelmi, Laser fur Ultrakurze Lichtimpulse, Akademi-Verlag, Berlin, 1984.
[7] K. Nagamuna, K. Mogi, H. Yamada, General method for ultrashort light pulse chirp measurement, IEEE J. Quantum Electron. 25 (1989) 1225–1233.
[8] J.P. van der Ziel, The mode-locking in semiconductor lasers, in: W.T. Tsang (Ed.), Semiconductors & Semimetals, Lightwave Communication Technology, vol. 22, Academic Press, Orlando, 1985, Chapter 1.